A Numerical Study on the Influence of CO_2 Addition on Soot Formation in an Ethylene/Air Diffusion Flame

Hongsheng Guo, Gregory J. Smallwood

Institute for Chemical Process and Environmental Technology
National Research Council Canada
1200 Montreal Road, Ottawa, Ontario, Canada K1A 0R6

1 Introduction

It has been confirmed that the addition of CO_2 to a diffusion flame suppresses the formation of soot. However, a consensus has not been reached regarding the mechanism of the suppression, especially the chemical effect. Some researchers claimed that the effect of CO_2 addition on soot formation is primarily due to the thermal and dilution effects [1], while others argued that there is also noticeable chemical effect [2-7]. Among the later group, some of them thought that the chemical effect is primarily caused by the enhanced soot oxidation process [2,3], while others believed that the chemical suppression is also a result of the reduced concentration of soot precursors and atomic hydrogen [4,7].

Most previous studies on the effect of CO_2 addition on soot formation were conducted by experiments [1-3, 5, 6]. Although experiments can capture the natural phenomena, it is hard to separate the coupled effects of different mechanisms. Numerical simulation has an advantage to separate the different mechanisms. However, in the past, usually simplified soot models were employed, or soot was totally neglected in the simulation [4], because of the limit of computation power and the lack of detailed soot formation model.

Significant progress has been made in the development of relatively detailed soot formation models. These models can capture many phenomena of soot formation in various flames. This paper further investigates the effect of CO_2 addition on soot formation in a laminar diffusion flame by numerical simulation using a relatively detailed soot model. The purpose is to use the details from numerical results to identify if there is chemical effect and how the chemical effect suppresses soot formation, when CO_2 is added to a laminar diffusion flame. The paper focuses on the fuel side addition, i.e. CO_2 is added to the fuel stream.

2 Numerical Model

The base flame studied was a coflow laminar ethylene/air diffusion flame experimentally studied by [8]. The governing equations for conservation of mass, momentum, energy and gas species mass fractions can be found elsewhere [9]. The gas phase reaction scheme and soot model used were basically those developed by Appel et al. [10]. Several modifications were made, since the original model underpredicted soot from the base flame.

The first modification was to limit the particle coagulation by setting the coagulation rate as zero when the mean particle diameter is greater than 25 nm. This was based on the experimental observation that generally the maximum diameter of a primary particle is about 25 nm. Then we increased the surface growth rate by changing the acetylene addition rate (S4 in the table 3 of [10]) and the parameter α – the fraction of surface sites available for surface reactions. The reaction rate of acetylene addition provided in [10] was increased by five times in this paper. The parameter α was still calculated by the Eq. 1 of [10], but the parameter a in the equation was

increased by 3 times and the parameter b was modified to $b = -1.38 + 1.02 \times 10^{-3} \times T$, with T being local temperature.

After above modifications, the peak soot volume fraction of the base flame was successfully predicted. However, soot volume fraction in the centerline region was still significantly underpredicted. Realizing that the chemistry developed in [10] underpredicted the concentration of pyrene (the inception PAH species) in some flames, we reduced the scrubbing factor of pyrene α_{A4} to 0.0005, i.e. the reaction rate of pyrene was calculated by $r_{A4} = r_{g,A4} + \alpha_{A4} \cdot r_{s,A4}$, where r_{A4}, $r_{g,A4}$, $r_{s,A4}$ and α_{A4} are, respectively, the net rate, the rate due to gas phase reactions, the rate due to soot formation and the scrubbing factor of pyrene. This treatment was an ad hoc one. The scrubbing factors for all other species were 1.0.

Other details of the soot model were the same as those in [10]. The free molecular regime was employed for the calculation of coagulation. The computational domain covered a region from 0 to 3.0 cm in the radial direction and 0 to 11.0 cm in the axial direction. The inflow boundary (z = 0 cm) corresponded to the region immediately above the fuel nozzle.
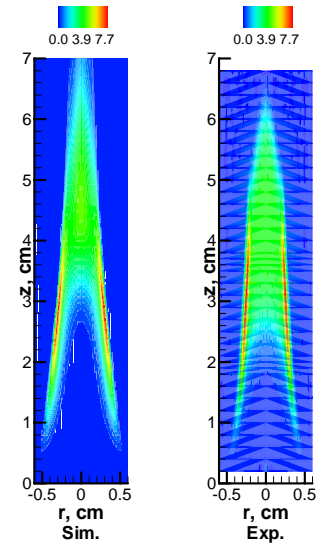

Fig. 1 Predicted and measured soot (ppm) in the base flame.

3   Results and Discussion

Figure 1 shows the comparison of soot volume fraction between the predicted by this paper and the measured by Gülder et al. [8] for the base flame. It is observed that the simulation basically captured the primary feature of soot in the base flame. Therefore, the model was used to investigate the effect of CO_2 addition. The mass flow rates of ethylene and air were kept constant, when CO_2 was added to the fuel side of the base flame.
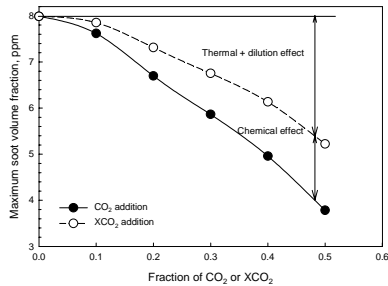

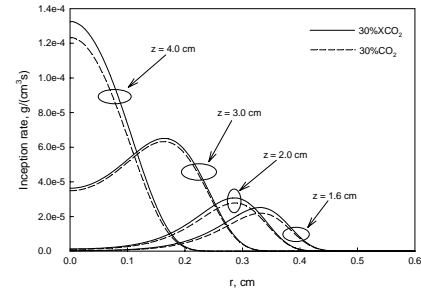Fig. 2 Variation of peak soot volume fraction.

Fig. 3 Inception rate.

Figure 2 shows the variation of the peak soot volume fraction with the change of the mole fraction of CO_2. It is observed that being consistent with the previous studies, the addition of CO_2 suppresses the formation of soot.

To identify the relative contribution of the chemical effect, the strategy used in our previous study was employed. In addition to the normal calculation, an extra one was carried out for each CO_2 diluted flame. In this extra calculation, the added CO_2 was replaced by an artificial species XCO_2, which had the same thermal and transport properties as CO_2, but was chemically inert. Therefore, the difference between the results of the normal and extra calculations reflects the chemical effect of CO_2 addition. The peak soot volume fractions in the XCO_2 diluted flames are also shown in Fig. 2. It is found that compared to the XCO_2 addition, the CO_2 addition further significantly reduces the formation of soot. This supports the argument that the addition of CO_2 suppresses soot

formation through not only the thermal and dilution effects, but also the noticeable chemical effect. This paper focuses on the chemical effect, since the thermal and dilution effects have been analyzed by many previous studies. We identify the chemical effect by comparing the results of 30%CO$_2$ and 30%XCO$_2$ diluted flames below.

Figures 3 and 4 display the soot inception and surface growth rates. It is revealed that both inception and surface growth rates in the CO$_2$ diluted flame are lower than in the XCO$_2$ diluted flame, meaning that the chemical effect of CO$_2$ addition suppresses both inception and surface growth processes.
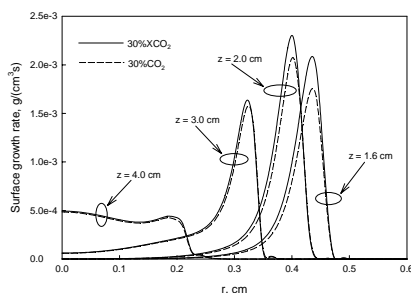

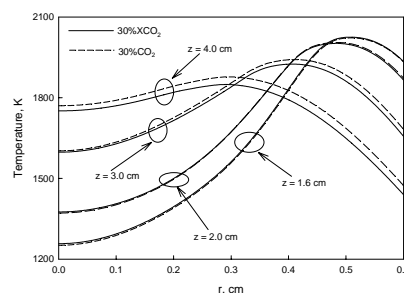Fig. 4 Surface growth rate.

Fig. 5 Temperature distribution.

In this paper, the particle inception is assumed to be due to the coagulation of two large PAH – pyrene. Therefore, the inception rate depends on temperature and pyrene concentration. Figures 5 and 6 give the distributions of temperature and concentration of pyrene. We can observe that at lower flame region, the difference in temperature between the CO$_2$ and XCO$_2$ diluted flames is negligible, while the flame temperature in the CO$_2$ diluted flame is higher in upper flame region. This suggests that temperature is not a factor that results in the lower soot inception rate in the CO$_2$ diluted flame. On the other hand, Fig. 6 shows that the concentration of pyrene is lower in the CO$_2$ diluted flame. Accordingly, the addition of CO$_2$ chemically reduces the concentration of pyrene and thus results in the lower particle inception rate in the CO$_2$ diluted flame. The higher temperature in the upper region of the CO$_2$ diluted flame is because of the lower soot volume fraction.
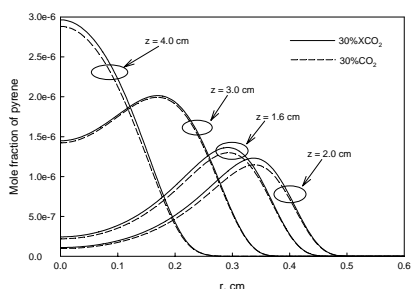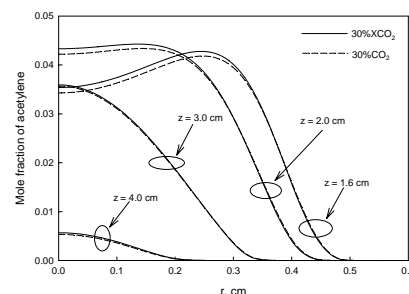

Fig. 6 Mole fraction of pyrene.

Fig. 7 Mole fraction of acetylene.

Surface growth is caused by PAH condensation and C$_2$H$_2$ addition. However, the calculation indicates that the PAH condensation rate is about one order of magnitude smaller than the C$_2$H$_2$ addition rate, meaning that C$_2$H$_2$ addition dominates surface growth process. Based on the HACA mechanism [10], C$_2$H$_2$ addition rate mainly depends on temperature, surface area and the concentrations of C$_2$H$_2$ and H. Figure 3 suggests that particle number density and thus surface area in the CO$_2$ diluted flame are lower. Therefore, the lower concentration of pyrene is also a factor that results in the lower surface growth rate in the CO$_2$ diluted flame. However, Fig. 5 shows that temperature is not a factor that leads to the lower surface growth rate in the CO$_2$ diluted flame.

Figure 7 displays the distribution of C$_2$H$_2$. It shows that although the concentration of C$_2$H$_2$ in the centerline region is lower in the CO$_2$ diluted flame, the difference is negligible in the surface growth region (see Fig. 4). Therefore, C$_2$H$_2$ is not a factor either causing the lower C$_2$H$_2$ addition rate in the CO$_2$ diluted flame.

Another factor that affects the C$_2$H$_2$ addition rate is the concentration of H, since it affects the hydrogen abstraction in HACA mechanism. The concentration of H is shown in Fig. 8. In the lower flame region, the concentration of H is lower in the CO$_2$ diluted flame, leading to the lower C$_2$H$_2$ addition rate there. In the upper flame region, although the peak concentration of H in the CO$_2$ diluted flame is similar to or higher than that in the XCO$_2$ diluted flame, the difference is negligible in the surface growth region. The lower surface growth rate in the upper flame region of the CO$_2$ diluted flame is caused by the lower surface area resulted from the lower inception rate. Therefore, we can conclude that the lower soot formation rate in the CO$_2$ diluted flame than in the XCO$_2$ diluted flame is because of the lower concentrations of pyrene and H. In other word, the chemical suppression effect of CO$_2$ addition on soot formation is because of the reduced concentrations of pyrene and H. The higher concentration of H in the upper region of the CO$_2$ diluted flame is caused by the higher temperature.
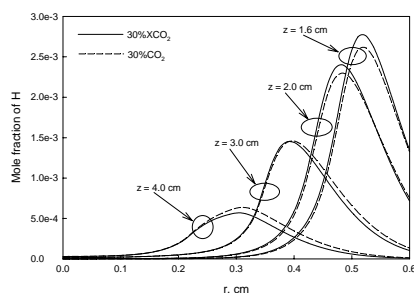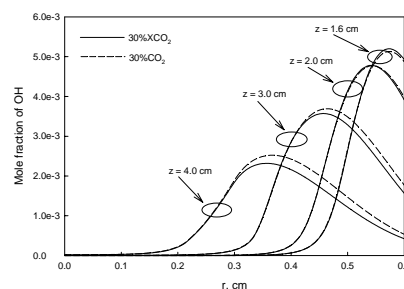

Fig. 8 Mole fraction of H.

Fig. 9 Mole fraction of OH.

The lower concentration of H in the lower region of the CO$_2$ diluted flame is because of the reaction CO + OH $\Leftarrow$ CO$_2$ + H, which enhances the consumption rate of H when CO$_2$ is added. The lower concentration of H also causes the lower growth rate of PAH, since H plays an important role in the growth of PAH. Therefore, the lower concentration of pyrene in the CO$_2$ diluted flame is also caused by the lower concentration of H. Accordingly, the lower concentration of H is the primary factor that causes the lower inception and surface growth rates in the CO$_2$ diluted flame.

Some researchers argued that the chemical suppression effect of CO$_2$ addition on net soot formation is that the soot oxidation is enhanced. The concentration of OH, the primary radical attacking soot, is displayed in Fig. 9. It is found that the difference in the concentration of OH in the CO$_2$ and XCO$_2$ diluted flames is negligible in the lower flame region. Although the peak OH concentration in the upper flame region of the CO$_2$ diluted flame is higher (resulting from the higher temperature), the difference is negligible near the centerline region where most soot is located. Therefore, the chemical effect of CO$_2$ addition on soot oxidation should be negligible.

4 Concluding Remarks

The effect of CO$_2$ addition on soot formation in an ethylene/air diffusion flame has been investigated by numerical simulation, with the focus on the chemical effect of CO$_2$ addition. A detailed gas phase chemistry and relatively detailed soot model have been employed. The result indicates that the addition of CO$_2$ does suppress soot formation through not only the thermal and dilution effects, but also the chemical effect. The chemical suppression effect of CO$_2$ addition on soot formation is primarily through reducing the concentration of radical H, which, in turn, decreases the rates of PAH and soot surface growth. The reduction of H concentration is caused by the reaction CO + OH $\Leftarrow$ CO$_2$ + H, which enhances the consumption rate of H, when CO$_2$ is added.

References

[1] Schug, K.P., Manheimer-Timnat, Y., Yaccarino, P., and Glassman, I. (1980). Sooting behavior of gaseous hydrocarbon diffusion flames and the influence of additives. Combust. Sci. Tecnol. 22: 235.

[2] Du, D.X., Axelbaum, R.L., and Law, C.K (1990). The influence of carbon dioxide and oxygen as additives on soot formation in diffusion flame. Proc. Combust. Inst. 23: 1501

[3] McLintock, I.S. (1962). The effect of various diluents on soot production in laminar ethylene diffusion flames. Combust. Flame 12: 217

[4] Liu, F., Guo,, H., Smallwood, G.J., and Gülder, Ö. L. (2001). The chemical effects of carbon dioxide as an additive in an ethylene diffusion flame: implications for soot and NOx formation. Combust. Flame 125: 778

[5] Gülder, Ö. L. and Baksh, M. F. (1993). Influence of carbon dioxide dilution on soot formation in diffusive combustion. Combustion Institute/ Canadian Section, Spring Technical Meeting, May 10-12, 1993, Université Laval, Québec.

[6] Oh, K.C., and Shin, H.D. (2006). The effect of oxygen and carbon dioxide concentration on soot formation in non-premixed flames. Fuel 85: 615

[7] Angrill, O., Geitlinger, H., Streibel, T., Suntz, S., and Bockhornm, H. (2000). Influence of exhaust gas recirculation on soot formation in diffusion flames. Proc. Combust. Inst. 28: 2643

[8] Gülder, Ö.L., Snelling, D.R., and Sawchuk, R.A. (1996). Influence of hydrogen addition to fuel on temperature field and soot formation in diffusion flames. Proc. Combust. Inst. 26: 2351

[9] Guo, H., Liu, F., Smallwood, G.J., and Gülder, Ö.L (2002). The flame preheating effect on numerical modelling of soot formation in a two-dimensional laminar ethylene-air diffusion flame. Combust. Theory Modelling 6: 173

[10] Appel, J., Bockhorn, H., and Frenklach, M. (2000). Kinetic modelling of soot formation with detailed chemistry and physics: laminar premixed flames of C$_2$ hydrocarbons. Combust. Flame 121: 122